

***N*-hydroxyphthalimide incorporated onto Cu-BTC metal organic frameworks: An novel catalyst for aerobic oxidation of toluene**

Li Bao¹ · Xingxing Li¹ · Zhaowei Wu¹ ·
Xia Yuan¹ · He'an Luo¹

Received: 25 July 2015 / Accepted: 30 November 2015
© Springer Science+Business Media Dordrecht 2015

Abstract *N*-hydroxyphthalimide (NHPI) incorporated onto a Cu-based metal–organic framework [NHPI/Cu-BTC (BTC:1,3,5-benzenetricarboxylate)] was prepared and used as a heterogeneous catalyst for aerobic oxidation of toluene under solvent-free conditions. Cu-BTC was synthesized through a hydrothermal and a solvothermal method with modification. The NHPI/Cu-BTC catalysts were synthesized by an impregnation method and characterized by scanning electron microscopy, X-ray diffractometry, Fourier transformed infrared spectroscopy, thermogravimetric analysis, and nitrogen adsorption. Results show NHPI was successfully incorporated onto Cu-BTC metal organic frameworks. The NHPI/Cu-BTC showed high catalytic performance in the aerobic oxidation of toluene. In the presence of 1 mol% NHPI/Cu-BTC and absence of any co-catalyst or co-solvent, the toluene oxidation was conducted at 110 °C for 2 h with 7.6 % conversion and more than 50 % benzaldehyde and benzyl alcohol selectivity. The structure stability of the catalysts after recovery was also studied.

Keywords Metal–organic framework · *N*-hydroxyphthalimide (NHPI) · Aerobic oxidation of toluene · Solvent-free

Introduction

The toluene oxidation is an important transformation in the chemical industry because the major products including benzaldehyde, benzyl alcohol, and benzoic acid are widely used to synthesize a diversity of useful chemicals, such as pharmaceuticals, dyestuffs, perfume, foodstuffs, preservatives, and rubber auxiliary

✉ Xia Yuan
yxiamail@163.com

¹ School of Chemical Engineering, Xiangtan University, Xiangtan City 411105, Hunan, People's Republic of China

agents [1, 2]. Nowadays, benzaldehyde and benzyl alcohol are more valuable than benzoic acid, and are especially needed in the industry. Currently, benzaldehyde is commercially prepared from the chlorination of toluene and then hydrolysis, which leads to some serious problems such as equipment corrosion and environmental pollution. Moreover, the resulting product is limited to synthesizing some high-quality compounds such as perfumes or pharmaceuticals for the inevitable production of chlorine [3, 4]. As reported, the direct oxidation from toluene to benzaldehyde is an environment-friendly method, and the resulting chlorine-free product can be used in perfumes and pharmaceuticals. In industry, caprolactam is synthesized from the SNIA process. In this process, toluene oxidation, as the first step, is carried out at 165 °C and 1.0 MPa catalyzed by cobaltous salts [5]. In addition, toluene is a starting material with the conversion of 14–15 %, which is mostly oxidized to benzoic acid with only a trace amount of benzaldehyde and benzyl alcohol (BD + BA) formed as by-products [6]. Therefore, the controlled oxidation from toluene to BD + BA using new catalytic materials under mild conditions has attracted much attention.

N-hydroxyphthalimide (NHPI) used in autoxidation reactions was first reported in 1986 [7]. Later it was reported that NHPI can be combined with transition metal salts in the presence of oxygen to efficiently oxidize alkanes [8], alcohols [9], and alkylaromatics [10] into the corresponding carbonyl compounds and/or carboxylic acids. Naturally, the new catalytic system combining NHPI with metal salts [11, 12], which served as radical catalysts, was used in the oxidation of toluene. It was proposed that a phthalimide *N*-oxyl (PINO) radical can be generated from NHPI in the presence of metal salts under mild conditions [13], while the carbon radicals derived from toluene under dioxygen led to oxygenation of compounds into benzaldehyde, benzyl alcohol, and benzoic acid as well as some by-products. This novel catalytic system with high conversion and suitable selectivity in oxidation of toluene would produce benzoic acid as the major final product. As reported, 2 % benzaldehyde and 81 % benzoic acid were produced in the presence of 10 mol% NHPI and 0.5 mol% Co(OAc)₂ in acetic acid under an oxygen atmosphere at 25 °C for 20 h [10]. Moreover, the oxidation of toluene after 12 h at 90 °C showed >95 % high conversion and >99 % benzoic acid selectivity, in the presence of 1 mol% NHPI, 1 mol% CoCl₂·6H₂O, and 0.5 mol% didecyldimethyl-ammonium bromide (DDAB) with a continuous flow of oxygen [14]. Toluene was efficiently transformed with 70.9 % conversion and 93.5 % selectivity to benzoic acid at 90 °C within 2 h in the presence of 5 mol% *N*-hydroxyquinolinimide (NHQI), 2.5 mol% CuCl₂ combined with hydroxypyrrolo [3,4-*b*]pyrazine-5,7-dione (HPPDO), and 7 mL of acetonitrile under oxygen [15].

Metal–organic frameworks (MOFs) are porous crystalline materials, and their structures are composed of transition metal ions (or clusters) that are connected to bi- or tri-podal rigid organic linkers [16–18]. MOFs have attracted wide attention owing to the highest porosities, world-record surface areas, and wide chemical inorganic–organic composition [19]. MOFs are widely used in gas storage [20], gas purification and separation applications [21], magnetism [22], sensors [23], as well as heterogeneous catalysis [24–26] owing to their special structural characteristics. As reported, a highly-active Fe-containing MIL-101 material was prepared and used

as a heterogeneous catalyst for oxidation of alcohols and alkenes [27]. A metal organic framework encapsulated with gold nanoparticles (noted as Au/UIO-66) was developed and used for selective oxidation of benzyl alcohol [28]. Palladium chloride was successfully immobilized on MOF-253 and proved to be a highly-active heterogeneous catalyst for Suzuki–Miyaura and Ullmann-type coupling reaction [29]. As an example of this classical material, Cu-BTC [BTC:1,3,5-benzenetricarboxylate $\text{Cu}_3(\text{BTC})_2$, or HKUST-1], which is generated by interconnection of $[\text{Cu}_2(\text{O}_2\text{CR})_4]$ units with a three-dimensional system, was first synthesized in 1999 [30]. Since then, the improved Cu-BTC synthesis method was reported [31–35]. Meanwhile, Cu-BTC was widely used in gas storage and gas separation [36–39] owing to the high porosity. Currently, owing to the large pore size, large surface area, and high metal content with active sites, the attention on application of Cu-BTC was transferred in catalysis. When cyanosilylation of benzaldehyde was used as a test reaction to study the catalytic properties of Cu-BTC, the removal of the Cu-bound water molecules allowed accessing the Lewis acid copper sites, which activated the reaction with a reasonable yield of 50–60 % after 72 h (313 K) [31]. Later, with the ethylene ketal of 2-bromopropiophenone as a test substrate, Alaerts et al. [40] proved that the active sites in Cu-BTC were hard Lewis acid sites and studied the adsorption CO and acetonitrile in IR spectroscopy supported as further evidence. Then Cu-BTC was used as a catalyst in the hydroxylation of toluene [41], Aldol condensation [42], chemical reduction of nitrophenol [43], oxidation of cyclooctene [44], and even oxygen reduction [45]. However, there are only a few reports about incorporating organic substrates onto Cu-BTC, which proved to be an effective catalyst in esterification [46] and Knoevenagel condensation [47]. Herein, we report the combination of NHPI with Cu-BTC (NHPI/Cu-BTC) by an impregnation method and use the prepared catalyst as an effective heterogeneous catalyst into the solvent-free oxidation of toluene.

Experimental methods

Materials

Copper(II) nitrate trihydrate $[\text{Cu}(\text{NO}_3)_2 \cdot 3\text{H}_2\text{O}]$ (99.5 %) was purchased from GuangFu Technology Development Co., Ltd. (Tianjin, China). 1,3,5-benzenetricarboxylic acid [H_3BTC , 98 %] and NHPI (97 %) were purchased from Sinopharm Chemical Reagent Co., Ltd. (Shanghai, China). Other reagents and solvents used here were all analytical-grade reagents obtained from the vendors and used without further purification.

Characterization techniques

The morphologies of the synthesized products were investigated on a Jeol JSM-6610LV scanning electron microscope (SEM) equipped with a tungsten filament. Samples were sputtered with gold prior to analysis and spread on a carbon disc mounted to SEM aluminum pin stubs. Fourier transformed infrared spectroscopy

(FTIR) was recorded in KBr disks with a Thermo Nicolet 380 FT-IR spectrometer. Elemental microanalysis (EA) was determined using a Vario EL analyzer. A Thermo Jarrell Asch IRIS Advantage 1000 inductively coupled plasma (ICP)-atomic spectroscopy was used to analyze metal contents. X-ray diffraction (XRD) patterns were detected on a Rigaku D/MAX 2500 diffractometer at 45 kv, 250 mA for CuK α ($\lambda = 1.5418 \text{ \AA}$) radiation, with a step size of 0.02° in 2θ . Thermogravimetric analysis (TGA) was performed on a TGA/SDTA 851^e device under N₂ atmosphere from 303 to 1073 K, with a heating rate of 10 K min^{-1} . The Brunauer, Emmett and Teller (BET) surface area and pore volume were measured by analyzing the results of nitrogen adsorption at 77 K in a NOVA-2200e Quanta chrome apparatus. Prior to measurements of N₂ adsorption, all samples were out-gassed at 423 K for 24 h.

Preparation of Cu-BTC

Two synthesis methods were selected from a reported synthesis route [48]. The details of the synthesis procedure are as follows.

H₃BTC (1.9664 g, 0.009 mol) was dissolved in ethanol (20 mL) and Cupric nitrate trihydrate (4.48 g, 0.018 mol) was dissolved in deionized water (10 mL) in different beakers. Prior to transfer into a Teflon-lined stainless steel autoclave, the two solutions were mixed and stirred at 298 K for 16 h. Then the autoclave was placed into an oven and heated at 413 K for 48 h. After cooling to room temperature normally, the resulting blue crystals were filtered, washed thoroughly with deionized water, and finally dried at 358 K for 12 h. The obtained product is named as Cu-BTC-A.

H₃BTC (1.0 g, 4.8 mmol) was dissolved in 30 mL of a 1:1 mixture of ethanol/*N,N*-dimethylformamide (DMF). Cu(NO₃)₂·3H₂O (2.077 g, 8.6 mmol) was dissolved in 15 mL of water in another flask. The two solutions were then mixed and stirred for 10 min before transferring into a Teflon-lined stainless steel autoclave. Then the autoclave was placed into an oven and heated at 373 K for 10 h. Finally, the reaction vessel was cooled to room temperature normally. The resulting blue crystals were isolated by filtration and extracted with methanol for 12 h using a Soxhlet extractor to remove solvated DMF. The product was then dried at 303 K for 12 h and named as Cu-BTC-B.

Preparation of NHPI/Cu-BTC

This method is a modification from a previous work [49]. Cu-BTC (1.0 g) was activated under vacuum at 473 K for about 2 h. NHPI (210 mg) was dissolved in a mixed solution of 7 mL of dichloromethane and 3 mL of methanol or 10 mL of tetrahydrofuran (THF). The activated Cu-BTC was added to this solution, and the resulting suspension was heated at 313 or 338 K (the temperature was selected depending on the solvent) for 4 h. After the required time, the mixture was cooled, and the solvent was removed by rotary evaporation. The resulting NHPI/Cu-BTC was dried at 353 K for 2 h. Finally, we acquired four catalysts: NHPI/Cu-BTC-A-1, NHPI/Cu-BTC-A-2, NHPI/Cu-BTC-B-1, and NHPI/Cu-BTC-B-2, using different

Cu-BTC samples and solvents. The letters A or B present different Cu-BTC samples. The number 1 means that dichloromethane and methanol are chosen as solvents to dissolve NHPI, and the number 2 indicates that THF is used.

Catalytic procedure for oxidation of toluene

In a typical reaction, toluene (5 g, 55 mmol) together with an appropriate amount of catalyst NHPI/Cu-BTC [0.43 g, 1 mol%, mol%: n (catalyst)/ n (toluene)] were placed into a 50 mL Teflon-lined magnetically stirred autoclave equipped with a block heater and a thermometer. The reactions were carried out at the required temperature under a molecular oxygen atmosphere (1.6 MPa) for hours. After that, the catalyst was filtered and washed with chloroform thoroughly, and the reaction mixture analyzed on an Agilent gas chromatography (GC)-6820 device equipped with a 30 m \times 0.32 mm \times 0.5 mm HP-Innowax capillary column, with N₂ used as carrier gas.

Results and discussion

Characterization

NHPI was incorporated onto Cu-BTC by adsorption from solutions as described in the Experimental section, and the resulting NHPI/Cu-BTC materials were characterized by SEM, FT-IR, TGA, XRD, and N₂ adsorption.

We acquired light blue Cu-BTC-A and bright Prussian blue Cu-BTC-B, which were in accordance with a reported article [48]. The SEM images (Fig. 1) show that the two different Cu-BTC samples (1a–1b) are both octahedral crystals. Moreover, Cu-BTC-A (1a) is smoother and a few other small spherical particles are present, whereas Cu-BTC-B (1b) is cubic-shaped with sharp edges without any spherical-shaped particle. The results indicate that Cu-BTC-A synthesized at higher temperature is impurity for the formation of Cu₂O as by-product. The changes in color and morphology may be partly attributed to the differences in synthesizing temperature and post-treatment procedures [30, 32, 48]. The morphological structures of the synthesized four NHPI/Cu-BTC (1c–1f) materials are also shown in Fig. 1. Compared with the single Cu-BTC, the crystal structure of NHPI/Cu-BTC materials become less irregular, which may be attributed to the mixing and stirring during the synthesized procedure. Unexpectedly, the images show few distinctions using different solvents as reaction media.

The XRD patterns of both Cu-BTC products are shown in Fig. 2. All samples shows high crystallinity, and especially the diffraction peaks at $2\theta = 6.6^\circ, 9.4^\circ, 11.6^\circ, 13.4^\circ, 17.4^\circ, 19.0^\circ, 25.9^\circ$ can be indexed to crystalline Cu-BTC (Fig. 2). The strong diffraction peaks at $2\theta = 36.4^\circ$ are present in the products (2a–2c), but not in Samples (2d–2f), indicating that Cu-BTC-A contained a small amount of Cu₂O impurity [50]. It was proved that Cu₂O as a by-product was formed easier at high temperature [30]. In our cases, Cu-BTC-A was synthesized at a high temperature of 413 K. Neither sample showed the peaks at $2\theta = 35.5^\circ, 38.7^\circ$, indicating the

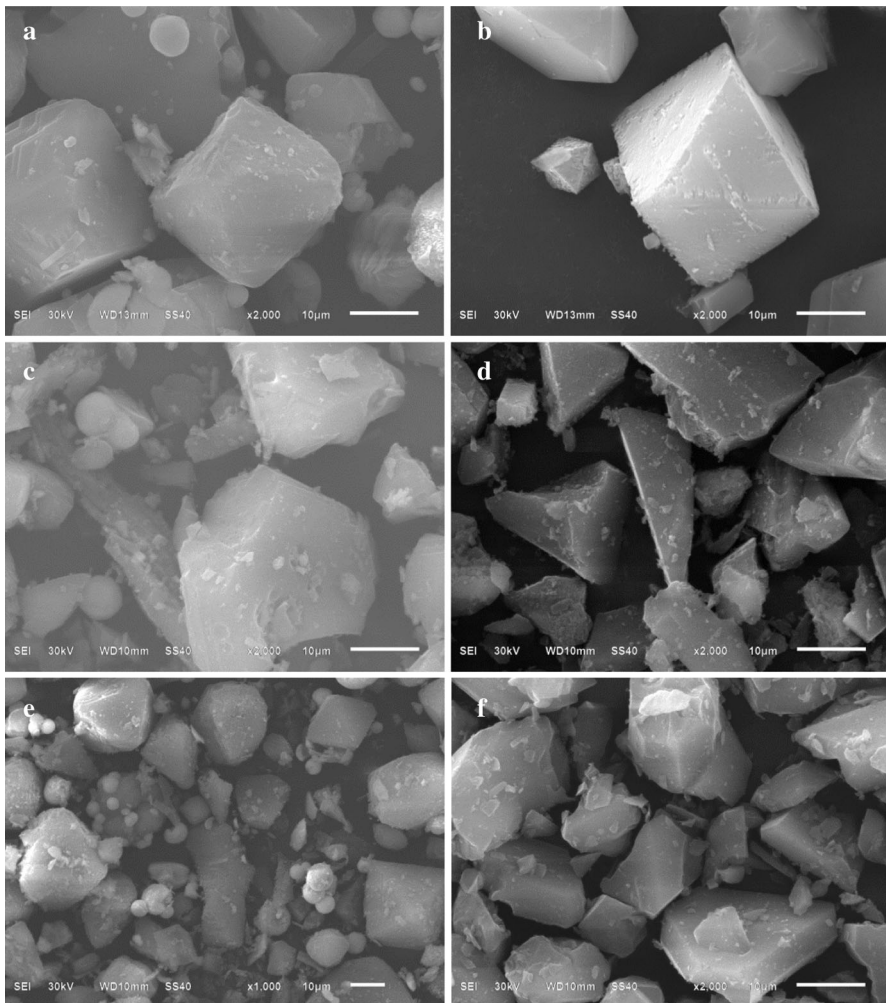


Fig. 1 SEM micrographs of products: **a** Cu-BTC-A; **b** Cu-BTC-B; **c** NHPI/Cu-BTC-A-1; **d** NHPI/Cu-BTC-B-1; **e** NHPI/Cu-BTC-A-2; **f** NHPI/Cu-BTC-B-2

product was CuO purity. Meanwhile, the diffraction peaks of NHPI/Cu-BTC materials in Fig. 2 were well consistent with Cu-BTC samples. It is clear that the incorporation of NHPI onto Cu-BTC did not change the crystal structure.

The thermal stability of synthesized Cu-BTC and NHPI/Cu-BTC products is presented in Fig. 3. The thermogram of Cu-BTC samples shows three regions. As for Cu-BTC-A (3e), the first weight loss (21 %) region between 303 and 433 K indicates the loss of moisture, the second region between 433 and 577 K shows a steady weight, and the third region starts at 577 K, where the structure of Cu-BTC collapses and the organic linker is buried. As for Cu-BTC-B (3f), the first region is between 303 and 443 K, with a weight loss about 33 % higher than that of Cu-BTC-

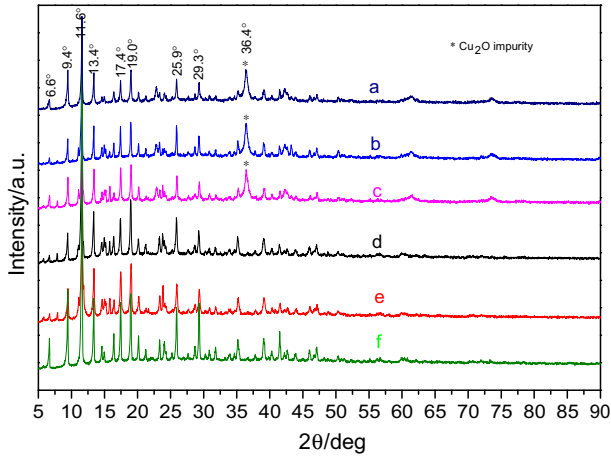


Fig. 2 XRD pattern of Cu-BTC and catalysts: *a* Cu-BTC-A; *b* NHPI/Cu-BTC-A-1; *c* NHPI/Cu-BTC-A-2; *d* NHPI/Cu-BTC-B-1; *e* NHPI/Cu-BTC-B-2; *f* Cu-BTC-B

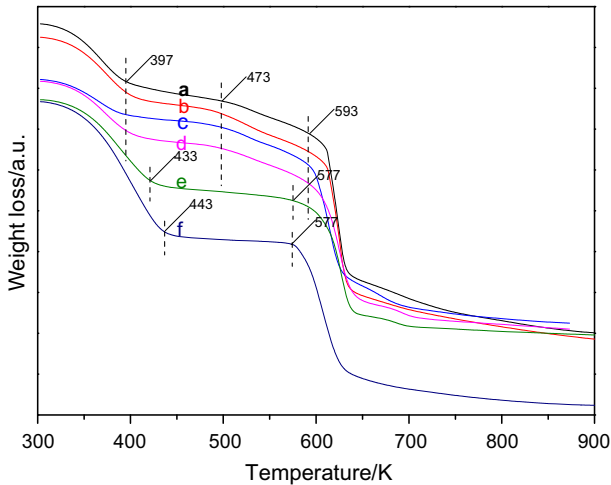


Fig. 3 TGA curve of Cu-BTC and catalysts: *a* NHPI/Cu-BTC-A-1; *b* NHPI/Cu-BTC-A-2; *c* NHPI/Cu-BTC-B-1; *d* NHPI/Cu-BTC-B-2; *e* Cu-BTC-A; *f* Cu-BTC-B

A, indicating the different contents of moisture or volatile solvent. The differences were attributed to post-treatment procedures used in preparation. Also, there is a steady weight from 443 to 577 K and the structure decomposed at above 577 K, finally forming CuO as the product. The same decomposition temperature at 577 K indicated the same thermal stability of the two samples. Obviously, NHPI/Cu-BTC catalysts had an additional weight loss, which contributed to the decomposition of NHPI at 473–593 K (Fig. 3a–d). The results undoubtedly indicate that NHPI was successfully incorporated onto the carrier Cu-BTC.

The BET surface area and pore volume of all samples are determined. The Cu-BTC-A has a surface area of $766 \text{ m}^2\text{g}^{-1}$ and a pore volume of $0.345 \text{ cm}^3\text{g}^{-1}$, while Cu-BTC-B has a surface area of $1404 \text{ m}^2\text{g}^{-1}$, which is twice as large as sample A, and a pore volume of $0.634 \text{ cm}^3\text{g}^{-1}$. After incorporation of NHPI, the surface area of Cu-BTC samples sharply decreased ($<30 \text{ m}^2\text{g}^{-1}$ in all NHPI/Cu-BTC samples), which was a significant evidence for the internal location of NHPI inside the carrier Cu-BTC.

The FT-IR patterns of all compounds are shown in Fig. 4. For both Cu-BTC samples, the presence of a broad and strong peak at 3454 cm^{-1} is assigned to ν (H_2O). The peak at 1641 cm^{-1} is assigned to ν ($\text{C}=\text{O}$) of the deprotonated H_3BTC . The peaks at 1373 and 1589 cm^{-1} are due to the ν_{sym} ($\text{C}-\text{O}_2$) and ν_{asym} ($\text{C}-\text{O}_2$) stretching modes, respectively. The IR bands around 729 and 1450 cm^{-1} are due to ($\text{C}-\text{H}$) bending mode and a combination of benzene ring stretching and deformation modes. The absorption bands around 500 cm^{-1} are assigned to ν ($\text{Cu}-\text{O}$) stretching modes [51]. The absence of the peak at 2970 cm^{-1} for sample B indicated the solvent DMF inside the channel of the compound was removed effectively by methanol as an extracted solvent [52]. As shown in Fig. 4, especially the bands at 1790 , 1722 , 1185 , 976 , and 882 cm^{-1} of NHPI/Cu-BTC indicated that NHPI was successfully incorporated onto Cu-BTC again. Theoretically, it is reasonable to assume that NHPI, with molecular size around 6.5 \AA , can be accommodated inside the intracrystalline space of Cu-BTC [49].

Finally, the element analysis results are showed in Table 1. The element contents of C and H both changed slightly between the two samples. However, Cu-BTC-A contains higher Cu content than Cu-BTC-B, which may be the key factor to the catalytic performance.

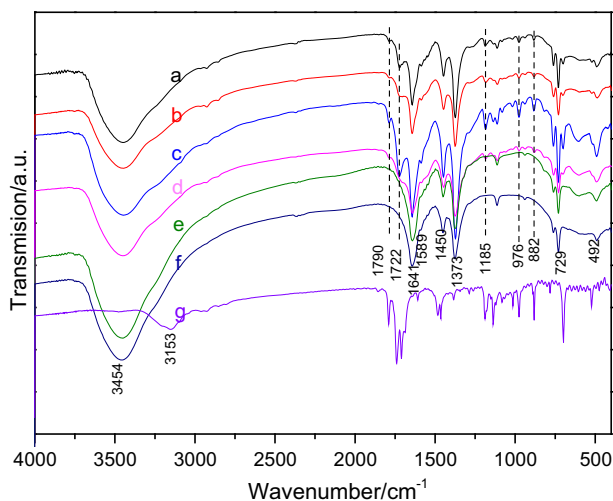


Fig. 4 FT-IR spectroscopy of materials: *a* NHPI/Cu-BTC-A-1; *b* NHPI/Cu-BTC-A-2; *c* NHPI/Cu-BTC-B-1; *d* NHPI/Cu-BTC-B-2; *e* Cu-BTC-A; *f* Cu-BTC-B; *g* NHPI

Table 1 The result of element analysis and inductively coupled plasma

Sample	C (%)	H (%)	Cu (%)
Cu-BTC-A ^a	25.0	3.2	36.7
Cu-BTC-B ^b	29.0	3.3	24.4

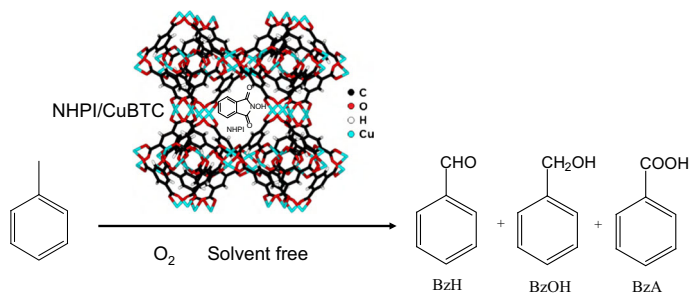
^a Sample synthesized at high temperature (413 K)

^b Sample synthesized at lower temperature (373 K)

Aerobic oxidation of toluene

NHPI in combination with metal salts was used as a heterogeneous catalyst for oxidation of toluene by using acetic acid as a solvent [10, 11]. Considering the solvent might cause environmental pollution, we used NHPI/Cu-BTC as a catalyst for selective oxidation of toluene (shown in Scheme 1) under solvent-free conditions and the catalytic performances are listed in Table 2.

Initially, the oxidation of toluene without catalyst or Cu-BTC (both Cu-BTC-A and Cu-BTC-B) alone under oxygen did not result in conversion. When NHPI acts as catalyst alone, the conversion of toluene is lower. However, NHPI adsorbed onto Cu-BTC was an active catalyst in the presence of oxygen at 110 °C, and NHPI/Cu-BTC catalysts showed different conversions of toluene and suitable BD + BA selectivity in 2 h in the absence of any co-solvent. When Cu-BTC-A was chosen as the carrier with different impregnation solvents for NHPI, the conversion rates of toluene were 7.7 and 7.6 %, respectively. On the contrary, the conversions of toluene were 5.8 and 5.4 % with Cu-BTC-B as the carrier. The negligible change may contribute to different contents of Cu, which was proved to be a co-catalyst in the oxidation [53]. Interestingly, when THF worked as a solvent for the synthesis of NHPI/Cu-BTC, the selectivity degrees of BD + BA are higher than that of dichloromethane and methanol used in the procedure (Table 2, Entry 4, 5, 6, 7). In contrast to NHPI/Cu-BTC, two control experiments were performed using a physical mixture of Cu-BTC and NHPI in the same ratio as an incorporated catalyst. Cu-BTC-A results in an 8.2 % conversion with 57.3 % BD + BA selectivity, and Cu-BTC-B yielded a 7.9 % conversion with 52.9 % of BD + BA selectivity.



Scheme 1 Aerobic oxidation of toluene using NHPI/Cu-BTC as catalyst

Table 2 Catalytic performance for aerobic oxidation of toluene

Entry	Catalysts	Conversion (%)	S _{BzH} (%)	S _{BzOH} (%)	S _{BzA} (%)
1	None	–	–	–	–
2	Cu-BTC	–	–	–	–
3	NHPI ^a	2.9	66.3	18.5	15.2
4	NHPI/Cu-BTC-A-1 ^c	7.7	41.1	8.9	50.0
5	NHPI/Cu-BTC-A-2	7.6	44.1	11.0	44.9
6	NHPI/Cu-BTC-B-1	5.8	45.7	6.6	47.7
7	NHPI/Cu-BTC-B-2	5.4	54.2	8.0	37.8
8	NHPI + Cu-BTC-A	8.2	43.3	14.0	42.7
9	NHPI + Cu-BTC-B	7.9	42.4	10.5	47.1
10	NHPI/Cu-BTC-B-1 ^b	5.2	53.8	3.9	42.3
11	NHPI/Cu-BTC-B-1 ^c	4.3	65.1	3.0	31.9
12	NHPI + Cu(NO ₃) ₂ ·3H ₂ O ^d	9.2	37.3	8.7	43.3

Reaction conditions: toluene 5 g, catalyst 0.43 g (1 mol%), O₂ 1.6 MPa, 110 °C, 2 h

^a NHPI 0.09 g (1 mol%)

^b Reaction temperature 100 °C

^c Reaction temperature 90 °C

^d NHPI 0.09 g (1 mol%), Cu(NO₃)₂·3H₂O 0.34 g

^e The letters of A (synthesized at high temperature) or B (synthesized at lower temperature) presents different Cu-BTC samples. The number 1 means that dichloromethane and methanol are chosen as solvents to dissolve NHPI, and the number 2 indicates that tetrahydrofuran (THF) is used

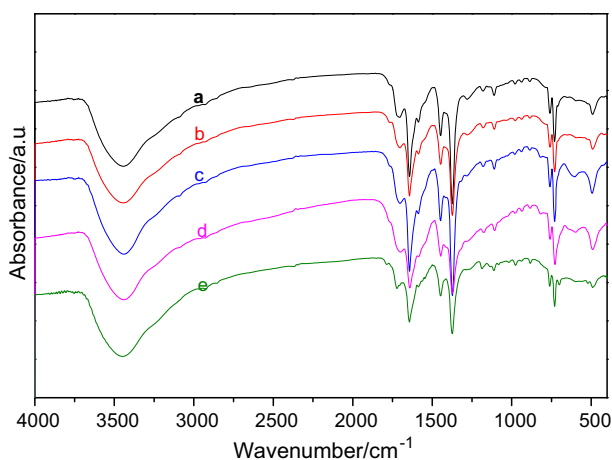


Fig. 5 FI-IR spectroscopy of fresh and recycled catalysts: *a* R-NHPI/Cu-BTC-A-1; *b* R-NHPI/Cu-BTC-A-2; *c* R-NHPI/Cu-BTC-B-1; *d* R-NHPI/Cu-BTC-B-2; *e* NHPI/Cu-BTC-A

To provide a qualitative assessment of catalytic performance of NHPI/Cu-BTC with respect to the analogous unsupported catalyst, we also performed an additional experiment with Cu(NO₃)₂·3H₂O in combination with the same molar ratio of NHPI

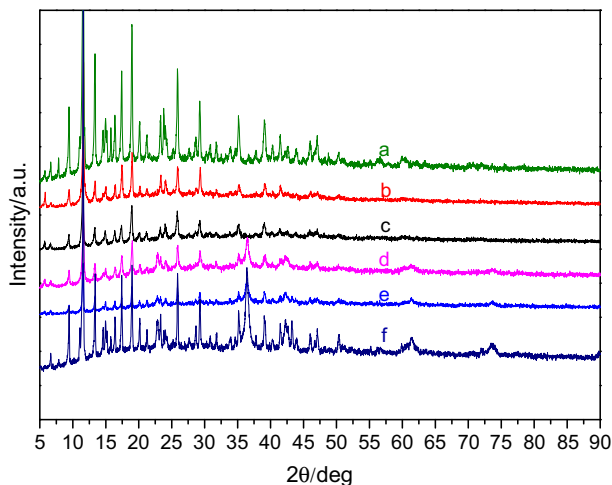


Fig. 6 Powder XRD pattern of fresh and recycled catalysts: *a* NHPI/Cu-BTC-A-1; *b* R-NHPI/Cu-BTC-A-1; *c* R-NHPI/Cu-BTC-A-2; *d* R-NHPI/Cu-BTC-B-1; *e* R-NHPI/Cu-BTC-B-2; *f* NHPI/Cu-BTC-B-1

as that of NHPI/Cu-BTC. As showed in Table 2, the reaction with $\text{Cu}(\text{NO}_3)_2 \cdot 3\text{H}_2\text{O}$ and NHPI resulted in 9.2 % conversion with 46.0 % of BD + BA selectivity in 2 h. In addition, some unidentified products were formed, which reduced the selectivity of the desired oxidation products. When the temperature decreased to 100 and 90 °C, the conversion was reduced to 5.2 and 4.3 %, respectively.

The structural stability of NHPI/Cu-BTC for the oxidation of toluene using molecular oxygen was investigated. After the first reaction, NHPI/Cu-BTC was obtained by filtration, washing with chloroform and oven-drying at 80 °C for 2 h. The structures of recycled catalysts are studied by FI-IR and XRD. As shown in Figs. 5 and 6, the peaks of the used catalysts are well consistent with the fresh ones, indicating the structures and perfect stability of the used NHPI/Cu-BTC catalysts are maintained under the reaction conditions.

Conclusions

We successfully incorporated NHPI onto two different Cu-BTC samples (NHPI/Cu-BTC), which were performed in controlled oxidation of toluene in the absence of additional co-solvents or additives under mild reaction conditions for the first time. The study shows that the reaction takes place with more than 50 % selectivity of BD + BA for 7.6 % conversion after 2 h at 110 °C in the presence of 1 mol% NHPI/Cu-BTC as catalyst. The catalysts could be separated from the reaction system by simple filtration and showed perfect stability. However, further studies are still necessary to optimize the catalytic performance of the prepared catalysts for toluene aerobic oxidation.

Acknowledgments This study was financially supported by the National Natural Science Foundation of China (No. 21376200), Hunan Provincial Natural Science Foundation of China (No. 14JJ2065), Hunan Provincial Colleges Innovation Platform Open Foundation (No. 13K044).

References

1. H.V. Borgaonkar, S.R. Raverkar, S.B. Chandalia, *Ind. Eng. Chem. Prod. Res. Dev.* **23**, 455 (1984)
2. H.-Y. Wu, X.-L. Zhang, X. Chen, Y. Chen, X.-C. Zheng, *J. Solid State Chem.* **211**, 51 (2014)
3. X. Li, B. Lu, J. Sun, X. Wang, J. Zhao, Q. Cai, *Catal. Commun.* **39**, 115 (2013)
4. L. Jia, S. Zhang, F. Gu, Y. Ping, X. Guo, Z. Zhong, F. Su, *Microporous Mesoporous Mater.* **149**, 158 (2012)
5. S. Tang, B. Liang, *Ind. Eng. Chem. Res.* **46**, 7826 (2007)
6. M. Xue, J. Ge, H. Zhang, J. Shen, *Appl. Catal. A Gen.* **330**, 117 (2007)
7. J. Föderier, C. Furbringer, K. Pfoertner, EP 0198351 (1985)
8. Y. Ishii, T. Iwahama, S. Sakaguchi, K. Nakayama, *J. Org. Chem.* **61**, 4520 (1996)
9. Y. Ishii, K. Nakayama, M. Takeno, S. Sakaguchi, T. Iwahama, Y. Nishiyama, *J. Org. Chem.* **60**, 3934 (1995)
10. Y. Yoshino, Y. Hayashi, T. Iwahama, S. Sakaguchi, Y. Ishii, *J. Org. Chem.* **62**, 6810 (1997)
11. J. Jiang, Y. Jing, Y. Zhang, N. Zhang, J. Jiao, W. Zhu, H. Xue, Y. Zong, G. Yang, *Catal. Lett.* **141**, 544 (2011)
12. Y. Ishii, *J. Mol. Catal. A Chem.* **117**, 123 (1997)
13. Y. Ishii, S. Sakaguchi, *Catal. Today* **117**, 105 (2006)
14. N. Taha, Y. Sasson, *Org. Process Res. Dev.* **14**, 701 (2010)
15. Q. Zhang, C. Chen, J. Xu, F. Wang, J. Gao, C. Xia, *Adv. Synth. Catal.* **353**, 226 (2011)
16. A. Dhakshinamoorthy, M. Opanasenko, J. Čejka, H. Garcia, *Adv. Synth. Catal.* **355**, 247 (2013)
17. S.L. James, *Chem. Soc. Rev.* **32**, 276 (2003)
18. H.C. Zhou, J.R. Long, O.M. Yaghi, *Chem. Rev.* **112**, 673 (2012)
19. A.U. Czaja, N. Trukhan, U. Müller, *Chem. Soc. Rev.* **38**, 1284 (2009)
20. S. Ma, H.-C. Zhou, *Chem. Commun.* **46**, 44 (2010)
21. J.-R. Li, R.J. Kuppler, H.-C. Zhou, *Chem. Soc. Rev.* **38**, 1477 (2009)
22. F.-H. Zhao, Y.-X. Che, J.-M. Zheng, *Inorg. Chim. Acta* **384**, 170 (2012)
23. D. Zhai, K. Zhang, Y. Zhang, H. Sun, G. Fan, *Inorg. Chim. Acta* **387**, 396 (2012)
24. J. Lee, O.K. Farha, J. Roberts, K.A. Scheidt, S.T. Nguyen, J.T. Hupp, *Chem. Soc. Rev.* **38**, 1450 (2009)
25. A. Dhakshinamoorthy, M. Alvaro, H. Garcia, *Catal. Sci. Technol.* **1**, 856 (2011)
26. S. Bhattacharjee, Y.R. Lee, P. Puthiaraj, S.M. Cho, W.S. Ahn, *Catal. Surv. Asia* **19**, 203 (2015)
27. A.M. Balu, C.S.K. Lin, H. Liu, Y. Li, C. Vargas, R. Luque, *Appl. Catal. A Gen.* **455**, 261 (2013)
28. J. Zhu, P.C. Wang, M. Lu, *Appl. Catal. A Gen.* **477**, 125 (2014)
29. L. Chen, Z. Gao, Y. Li, *Catal. Today* **245**, 122 (2015)
30. S.S.-Y. Chui, S.M.-F. Lo, J.P.H. Charmant, A. Guy Orpen, I.D. Williams, *Science* **283**, 1148 (1999)
31. K. Schlichte, T. Kratzke, S. Kaskel, *Microporous Mesoporous Mater.* **73**, 81 (2004)
32. Q.M. Wang, D. Shen, M. Bulow, M.L. Lau, S. Deng, F.R. Fitch, N.O. Lemcoff, J. Semanscin, *Microporous Mesoporous Mater.* **55**, 217 (2002)
33. D. Zacher, J. Liu, K. Huber, R.A. Fischer, *Chem. Commun.* **9**, 1031 (2009)
34. N.A. Khan, E. Haque, S.H. Jung, *Phys. Chem. Chem. Phys.* **12**, 2625 (2010)
35. Z.-Q. Li, L.-G. Qiu, T. Xu, Y. Wu, W. Wang, Z.-Y. Wu, X. Jiang, *Mater. Lett.* **63**, 78 (2009)
36. L.J. Murray, M. Dincă, J.R. Long, *Chem. Soc. Rev.* **38**, 1294 (2009)
37. S. Wang, Q. Yang, C. Zhong, *Sep. Purif. Technol.* **60**, 30 (2008)
38. J. Liu, J.T. Culp, S. Natesakhawat, B.C. Bockrath, B. Zande, S. Sankar, G. Garberoglio, J.K. Johnson, *J. Phys. Chem. C* **111**, 9305 (2007)
39. L. Hamon, E. Jolimaître, G.D. Pirngruber, *Ind. Eng. Chem. Res.* **49**, 7497 (2010)
40. L. Alaerts, F. Thibault-Starzyk, E. Séguin, J.F. Denayer, P.A. Jacobs, D.E. De Vos, *Stud. Surf. Sci. Catal.* **170**, 1996 (2007)
41. S. Marx, W. Kleist, A. Baiker, *J. Catal.* **281**, 76 (2011)
42. N.B. Pathan, A.M. Rahatgaonkar, M.S. Chorghade, *Catal. Commun.* **12**, 1170 (2011)

43. R. Senthil Kumar, S. Senthil Kumar, M. Anbu Kulandainathan, *Microporous Mesoporous Mater.* **168**, 57 (2013)
44. U. Junghans, C. Suttkus, J. Lincke, D. Lässig, H. Krautscheid, R. Gläser, *Microporous Mesoporous Mater.* **216**, 151 (2015)
45. J. Mao, L. Yang, P. Yu, X. Wei, L. Mao, *Electrochem. Commun.* **19**, 29 (2012)
46. L.H. Wee, N. Janssens, S.R. Bajpe, C.E.A. Kirschhock, J.A. Martens, *Catal. Today* **171**, 275 (2011)
47. Q.-X. Luo, X.-D. Song, M. Ji, S.-E. Park, C. Hao, Y.-Q. Li, *Appl. Catal. A Gen.* **478**, 81 (2014)
48. P. Chowdhury, C. Bikkina, D. Meister, F. Dreisbach, S. Gumma, *Microporous Mesoporous Mater.* **117**, 406 (2009)
49. A. Dhakshinamoorthy, M. Alvaro, H. Garcia, *J. Catal.* **289**, 259 (2012)
50. S.N. Nobar, Adsorption and diffusion of gases in Cu-BTC, Sharif University of Technology, Tehran, (2013)
51. Y. Feng, H. Jiang, S. Li, J. Wang, X. Jing, Y. Wang, M. Chen, *Colloids Surf. A Physicochem. Eng. Asp.* **431**, 87 (2013)
52. Z. Xiang, D. Cao, X. Shao, W. Wang, J. Zhang, W. Wu, *Chem. Eng. Sci.* **65**, 3140 (2010)
53. G. Yang, L. Wang, J. Li, Y. Zhang, X. Dong, Y. Lv, S. Gao, *Res. Chem. Intermed.* **38**, 775 (2011)